The flow structure on drag-reduced riblet surfaces

FengBeibei   ChenDarong   WangJiadao

Abstract—The structure of air flow on riblet surfaces has been studied with direct numerical simulations. Drag reduction was achieved through optimization of riblet geometry affecting the flow structure in riblet grooves. Force analysis and flow structure is studied based on k-ε turbulence model, and drag reduction and increase mechanism on riblet surfaces is related to the flow alteration. Reynolds shear stress is significantly decreased which is considered the dominant factor resulting in drag reduction. Through force analysis, the significant decrease of viscous force is considered the dominant factor resulting in drag reduction.Pressure drag on riblet surfaces generating from the deviation of static pressure on the front and rear end of the riblet occurred and grew exponentially with the flow rate. Near-wall vortical structures, Reynolds shear stress, static pressure and velocity field on riblet surfaces is analyzed in detail.

Keywords—flow structure; riblet surfaces; drag reduction; microvortex ;viscous force

I. INTRODUCTION

Riblet surfaces on fluid drag reduction have been a field of intensive research due to its significant impact on energy saving and drag reduction. There are many engineering applications in aeronautics, marine, ground vehicles, and in pipelines as well those can be greatly benefited from any significant amount of drag reduction. Aiming at maximizing the net drag reduction, considerable efforts have been devoted to the theoretical understanding of drag reduction mechanisms and the development of an optimum shape of riblets. Suzuki and Garcia-Mayoral thought the mean velocity profile in viscous sublayer would be modified and played significant role on reducing the drag, and measured the velocity field in triangular riblet region [1]-[2].While, Vukoslavcevic and Park used hot-wires in their measurements [3]-[4]. Static pressure distribution in the riblet grooves should generate exclude additional forces in the streamwise direction [5]. Vortices induced in the riblet grooves (called "Second Vortex" theory in some references) are considered the most important factor to analyze the mechanism of the turbulent drag reduction over riblet surfaces [6]. The development of optimum shape of riblets has been carried on available from many laboratories. Different shapes including the triangular, rectangular, trapezoidal, sawtooth and scalloped cross-sections have been investigated through experiments and simulations [7]-[11]. But, numerical techniques have still lagged the experiments due to the lack of computational resources.

The objective of the present study is to propose a simple and accurate numerical treatment for the flow characteristics inside the riblet grooves of infinitesimal thicknesses less than the actual model size based on direct numerical simulation which is often adopted to study the flow characteristics for high-speed air flow [12].That is to avoid the heavy computational effort needed in mapping techniques and the excessive grid clustering near the riblet surfaces as well. The proposed technique is intended to be used for perpetual computations for different geometrical parameters while the flow rate ranges from 0.05Ma to 0.95Ma. For this purpose, a finite volume code is modified to reconstruct the cells near the riblet and a second-order upwind discretization is used in calculation at the new constructed surfaces. The reliability of the method is judged by comparing the results with those of experiments[13]. The underlying changes along with the flow rate inside riblet grooves are presented aiming at explaining the drag reduction and increase mechanisms.

II. NUMERICAL APPROACH

Direct numerical simulations based on k-ε turbulence model are conducted to study the characteristics of flow in thin triangular riblet grooves. The k-ε turbulence model was proved to be a useful tool for the understanding of mass transfer and Reynolds stress in momentum equation in turbulence boundary layer of high-speed air flow [14] compared with the k-ω turbulence model which is based easily on the method of the near wall function [15]. The flow characteristic is described by the distributions of velocity field, mass transfer, static pressure and Reynolds shear stress.

K-ε turbulence model calculates the numerical solution of Reynolds-averaged Navier-Stokes equations based on the balance of the generation and dissipation of turbulent kinetic energy. The relationship between eddy viscosity coefficient and turbulent kinetic energy together with the energy dissipation rate is needed as shown in Eq.(1).

Feng Beibei is with the State Key Laboratory of Tribology, Tsinghua University, Beijing, 100084 China (corresponding author; phone: (+86)13701254942;fax: (+86)010-62781379; e-mail: fbb07@mails.tsinghua.edu.cn).

Chen Darong is with the State Key Laboratory of Tribology, professor at Tsinghua University, Beijing, 100084 China(e-mail: chendr@mail.tsinghua.edu.cn).

Wang Jiadao is with the State Key Laboratory of Tribology, associate professor at Tsinghua University, Beijing, 100084 China(e-mail: jdwang@mail.tsinghua.edu.cn).

$$v_t = C_\mu \frac{k^2}{\varepsilon} \tag{1}$$

Where C_μ is dimensionless coefficient, k is turbulent kinetic energy, and ε is the dissipation rate of turbulent kinetic energy.

K-ε turbulence model is to solve the k equation and ε equation, then get the turbulent viscous stress η_t. To proceed, calculate the turbulent stress using the Boussinesq Hypothesis.

Eq.(1) is expressed as follow:

$$\eta_t = c_\mu \rho k^2 / \varepsilon \tag{2}$$

$$(\tau_{i,j})_t = -\frac{2}{3}\rho k \delta_{i,j} + \eta_t(\frac{\partial u_i}{\partial x_j} + \frac{\partial u_j}{\partial x_i}) \tag{3}$$

Turbulence pulsation kinetic-energy K is defined as

$$K = \overline{u_i' u_i'} / 2 \tag{4}$$

The dissipation rate of turbulent kinetic energy ε accounts for the transfer rate of mechanical energy into heat of isotropic small-scale vortices, and could be defined as

$$\varepsilon = v\overline{(\partial u_i' / \partial x_k')(\partial u_i' / \partial x_k')} \tag{5}$$

To solve the k equation and ε equation:
k equation:

$$\rho\frac{\partial K}{\partial t} + \rho u_j \frac{\partial K}{\partial x_j} = \frac{\partial}{\partial x_j}[(\eta + \frac{\eta_t}{\sigma_k})\frac{\partial K}{\partial x_j}] + \eta_t \frac{\partial u_i}{\partial x_i}(\frac{\partial u_j}{\partial x_i} + \frac{\partial u_i}{\partial x_j}) - \rho\varepsilon \tag{6}$$

ε equation:

$$\rho\frac{\partial \varepsilon}{\partial t} + \rho u_k \frac{\partial \varepsilon}{\partial x_k} = \frac{\partial}{\partial x_k}[(\eta + \frac{\eta_t}{\sigma_\varepsilon})\frac{\partial \varepsilon}{\partial x_k}] + \frac{c_1\varepsilon}{K}\eta_t \frac{\partial u_j}{\partial x_i}(\frac{\partial u_j}{\partial x_i} + \frac{\partial u_i}{\partial x_j}) - c_2\rho\frac{\varepsilon^2}{K} \tag{7}$$

To proceed, we integrate Eq.(6), Eq.(7) with turbulent momentum equation, and the unified form is the governing equations of k-ε turbulence model .Common calculation program is to solve the above governing equations.

III. TREATMENT OF CUT CELL

The challenge in the present study is to treat an infinitesimal body whose thickness is less than the nominal grid sizes. Schematic description of the problem is shown in Fig. 1.Such tiny riblets can be represented easily in rectangular coordinate system.To avoid the heavy computational effort needed in mapping techniques and the excessive grid clustering near the riblets surfaces as well, a modified calculation unit is adopted to the simulation of flow characteristics inside the riblet grooves as shown in Fig.1.
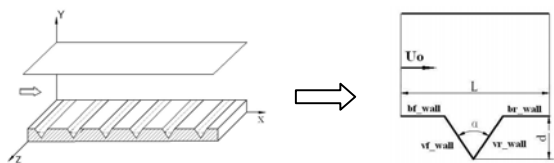
(a). Riblet surface   (b). Calculation unit
Fig.1 Computational domain

With the inclusion of the riblet surface and smooth surface inside the domain, the calculation unit is shown in Fig.1(b).Riblet surface is composed of bf_wall, vf_wall, vr_wall, and vf_wall. Respectively, the flow characteristic parameters on each part of the riblet surface should be obtained along with the flow rate.
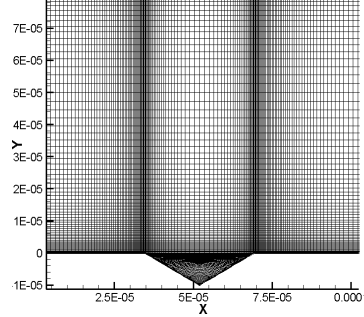

Fig.2 Transverse view of the numerical grid.

A transverse view of the numerical grid in the vicinity of the riblets is shown in Fig.2 for the thin triangular riblet surface.

IV. COMPUTATIONAL DETAILS

The computational domain has the dimensions 1.039230 e-004m × 1.0e-004m in x, y directions. Respectively, which is relatively larger than the minimal riblet groove unit. Due to the various geometrical parameters of the riblets, the riblets are described with four geometrical parameters. In this paper, nineteen cases have been studied with certain geometry while the flow rate ranges from 0.05Ma to 0.95Ma with interval of 0.05Ma. The calculating object has used 16875 cells, 34025 faces, and 17151nodes in the directions. Uniform meshes have been used in every calculation cases.

The number of grid points existing near the wall and inside the grooves is much larger than that of the flow gentle change region. The no-slip boundary conditions are applied at all cases. The turbulent flow is assumed fully developed over the riblets so that the Inlet/Outlet boundary conditions are simply assigned in the directions. The fluid material is defined as compressible gas, and its thermal conductivity is constant as 0.0242w/(m*k). The courant number is 200 in order to make the calculation fully convergent and high efficiency.
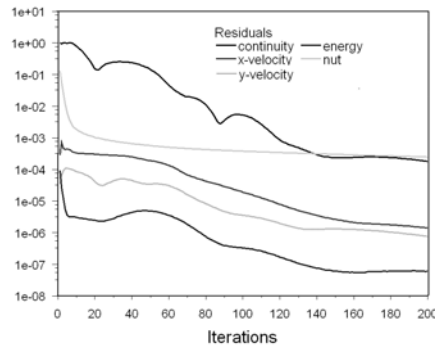

Fig.3. Residual monitors of continuity, x-velocity, y-velocity, energy and nut (convergence criterion) during calculation along with iterations.

In the calculation case with flow rate 0.20Ma, the residual values for each variable degrade below 1e-03, and we consider the calculation is fully convergent. The residual value curves of the flow characteristic parameters are presented in Fig.3.

V.   RESULTS AND DISCUSSIONS

A. Force Analysis

Force on riblet surfaces is analyzed in detail. Viscous force and pressure force is considered the two main forces on surface.On smooth surface, pressure drag is zero because no microvortical structure generates on smooth surface which will cause deviation of static pressure on the front and rear end of the riblets. Viscous force now is the total force, and due to the strong shear on smooth surface now skin friction is totally composed of viscous force. On riblet surfaces, an obvious phenomena is that microvortex will be induced in riblet grooves, which will greatly degrade the strong wall shear. And, viscous force resulting from the   shearing at solid-vapor interface is correspondingly decreasing, which is the main factor of drag-reduced riblet surfaces. Meanwhile, pressure drag which is caused by the deviation of static pressure, high pressure at the front end of riblets and low pressure zone at the rear end of riblets. And, it is related to the induced microvortex in riblet grooves. Microvortex will affect the static distribution and pressure drag, which can be affected by the riblet geometry.

Especially, at high-speed air flow the microvortex formed in riblet grooves will greatly affect the skin friction. Viscous force and pressure force is closely related to the characteristics of microvortex. So, it is necessary to study the microvortex on riblet surfaces.
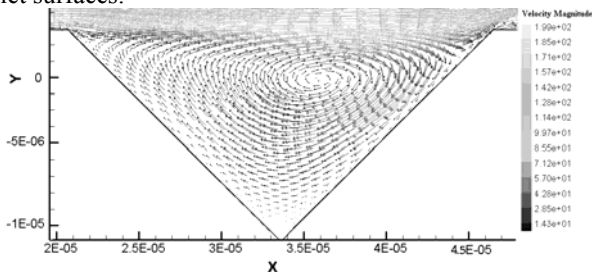

Fig.4 Microvortex induced in riblet grooves

Take the flow mach number is 0.8Ma for instance. Flow of microvortex is shown in Fig.4. Center of microvortex leans to the front end of riblet, which will result in high pressure zone at this area. The flow rate is 0.8Ma, and the average line speed of microvortex is about 42.8m/s-57.0m/s(estimated). High-speed rotation of microvortex is due to the energy and momentum transfer at the turbulence boundary layer. And the linear speed and wall shearing is greatly degraded compared with smooth surface, which results in the viscous drag reduction. Tabel.1 shows the force on smooth surface and riblet surface while 0.8M. On smooth surface, pressure force is zero while no static pressure distribution deviation and viscous force is about 0.1607N. So, total force on smooth surface is equal to viscous force,0.1607N.While on riblet surface, pressure force is about 0.0252N due to the static pressure distribution deviation and

viscous force is about 0.1313N which is obviously degraded compared with that on smooth surface. We can find out the total force is less than that of smooth surface. Riblet structure has significantly degraded the surface force.

Tab.1 Force analysis on riblet surface

Zone Name	Pressure Force（N）	Viscous Force（N）	Total Force（N）
Smooth Surface	0	0.16069686	0.16069686
Riblet Surface	0.025263131	0.13132645	0.15658958

B. Drag Reducing Case and Drag Increasing Case

The code was validated by simulation using the certain geometry riblet surface compared with the smooth surface. Wall friction generates from the intense shear when high-speed air flow over the wall. Joseph has emphasized that the fluid speeds in the drag reducing regime are comparable to the speed of shear wave propagation [16]-[17]. On riblet surface, the Reynolds shear stress is greatly decreased due to the effect of vortices induced inside riblet grooves as shown in Fig.4(a) and Fig.5(a).The valley in Fig.4(a) and Fig.5(a) shows the degraded zone of Reynolds shear stress to nearly zero while on smooth surface the value is almost 4e+0061/s(when position is 5e-005m) which was the dominant factor resulting in drag reduction. Meanwhile, riblet surfaces generate an additional force in the streamwise direction [5].The force is due to the dissipation of static pressure inside the grooves. A low pressure zone and a high pressure zone occur on riblet surface. The pressure differences result in the additional forces which is significantly related to the flow rate and the shape and size of riblets. The balance of drag reduction due to degradation of Reynolds shear stress and additional force resulted from pressure differences affect the wall friction up and down on triangular riblet surfaces.
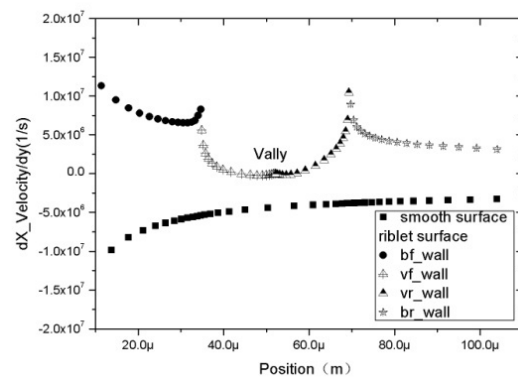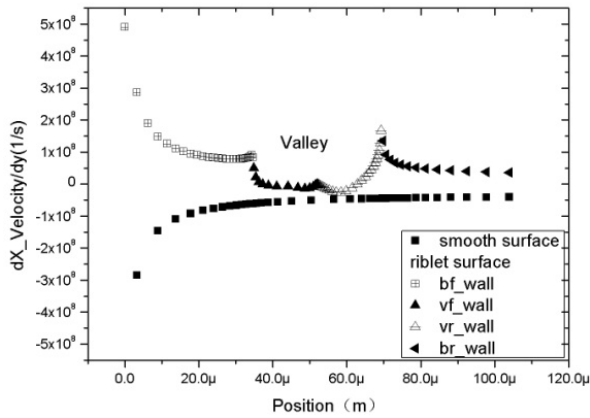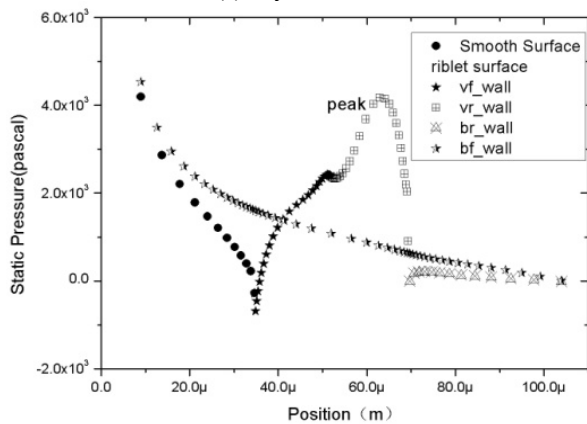

(a) Reynolds shear stress
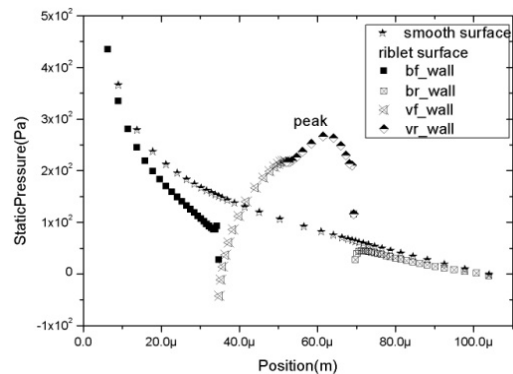
(b). Static pressure

Fig.5. Dissipation of Reynolds Shear Stress and Static Pressure on smooth and riblet surfaces at flow rate 0.1Ma (Drag reducing case).

Dissipation of Reynolds shear stress and static pressure in drag reducing case and increasing case have been shown in Fig.5 and Fig.6.In spite of the flow rate, Reynolds shear stress is obviously degraded. While, pressure difference shows expone- ntial growth along with the flow rate. The difference of peak(value is 9592.38Pa) and valley(value is 147.682Pa) of static pressure on riblet surface shown in Fig.6(b) is much bigger and the additional pressure drag is bigger than the decreased force due to the degradation of shear stress, which shows increasing drag totally.

(a) Reynolds shear stress

(b). Static pressure

Fig.6. Dissipation of Reynolds Shear Stress and Static Pressure on smooth and riblet surfaces at flow rate 0.6Ma (Drag increasing case).

C. Reynolds Shear Stress

Reynolds shear stress is plotted in Fig. 5(a) for the drag reduction case in which the stress is suppressed due to vortices induced in riblet grooves as shown in Fig.12 The value of the curve valley is nearly 5e+05(1/s) whereas on smooth surface the value is around 5e+06(1/s), which shows the stress is deeply weakened on riblet surface in drag decrease and drag increase cases, the curve valley of Reynolds shear stress is identical and shifted up at the end of grooves. So, shear stress could be greatly decreased due to riblets at any flow rate. The reason is considered related to the vortices induced in riblet grooves.

D. Static Pressure and Pressure Drag

Distribution of static pressure is modified over thin triangular riblet surface. High pressure zone and low pressure zone is verified located at several locations of riblet grooves, which results in the exclude additional forces on riblet surface. The force generates from the deviation of static pressures on the front and rear end of a riblet groove.

Fig.7 illustrates the distribution of wall static pressure on smooth surface and riblet surface at flow rate 0.4Ma. Regardless of the rate, it would be almost the same distribution of static pressure. In this simulation case, the value of center pressure of high pressure zone located at the rear end of groove is 4049.21 Pa, while the value of low pressure zone located at the front end is about 1791.4Pa. The additional force relies on the pressure difference which show significantly inconsistent in the drag reducing case and the drag increasing case.
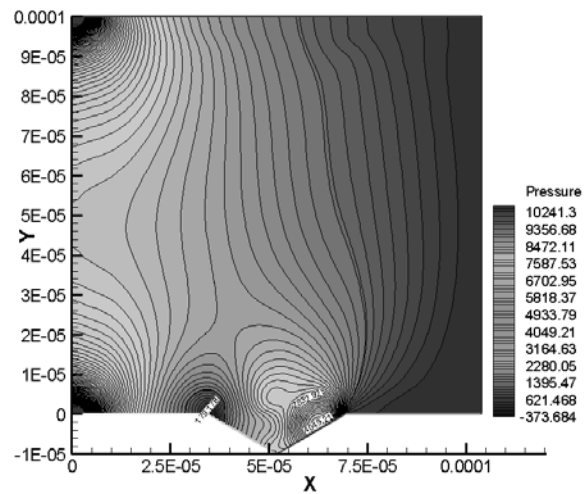

Fig.7 Distribution of wall static pressure on smooth surface and riblet surface at flow rate 0.4Ma.

The pressure values on riblet surface increase significantly with increasing of flow rate that plotted in Fig.8.
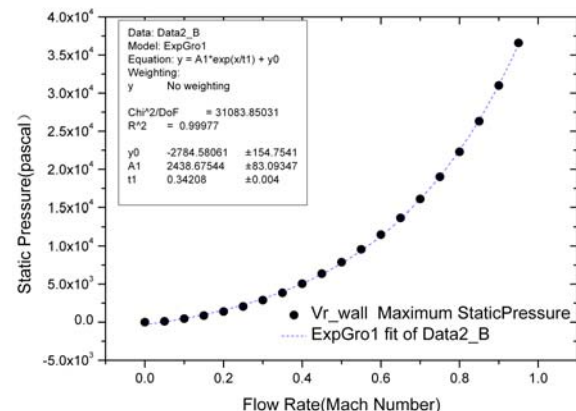

Fig.8 Growth of maximum static pressure in the center of high-pressure zone with flow rate from 0 to 0.95Ma.

Growth of static pressure with flow rate show exponential growth, and could be described with Eq.(6).

Equation: $y = A1*exp(x/t1) + y0$ (6)

Where A1 is 2438.7, and t1 is 0.34208, the value of y0 is

-2784.6 in this simulation case. A drag increasing trend, especially the pressure drag, exists due to the significant growth of static pressure along with the flow rate. In different simulation cases, the distribution of static pressure shows the same ,especially the exponential growth of center static pressure. It's no business with riblet geometry. But, the coefficients A1,t1,y0 are closely related to the riblet geometry. Different riblets affect the distribution of static. That is why to optimize the configuration parameters of riblets. Distribution of static pressure and pressure drag will change along with the shape and size of riblets.

Many researchers have explored the impact of riblet geometry on distribution of static pressure and surface drag reduction by using experiments, numerical simulation and theoretical analysis. Luchini et al [18] suggested that riblet surface can hamper the lateral component of the near-wall flow, and wall shear stress. Choi et al [19] supported this view by experimental and numerical investigations. But, most of the researchers were performed only to reduce the surface friction drag. For the riblet surface, the pressure drag resulting from the deviation of static pressure has an important effect on the drag of friction in high-speed air flow. Studies about optimization of riblet geometry to reduce pressure drag and drag reduction are widely done. The likely effects of shape and size of riblets on friction drag reduction have been assessed both by McLean et al.[20] and Walsh et al.[21].Riblets with certain optimized riblets were found to give nearly the same level of drag reduction as about 10-15% drag reduction while the flow rate ranging from 0.3M to 0.8M. While attitude angle of riblets which is the most factor to affect the distribution of static pressure and drag reduction on riblet surface haven't been system studied. Based on k-ε turbulence model and dynamic mapping techniques, we studied the distribution of static pressure on three different attitude angle of riblets and the impact on pressure drag reduction.Fig.9 shows the numerical calculation results. Distribution of static pressure greatly changed with riblet attitude angles. The high pressure zone located at the front end is closely related to riblet attitude angles. While flow rate is 0.7M, the value of high pressure center is 12758.8Pa with attitude angle -15°；that of 0° is 11560.6Pa while it is 13218.5Pa with attitude angle 15°.
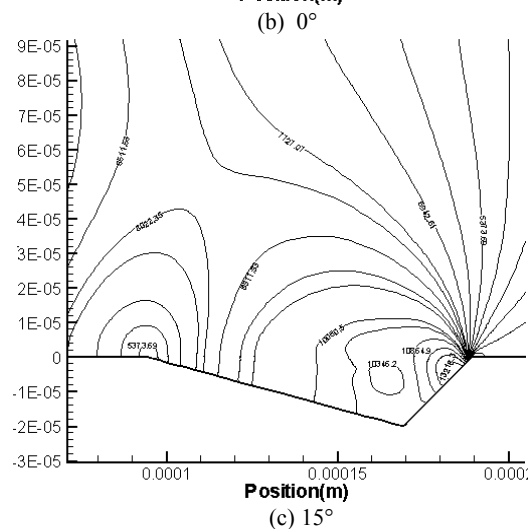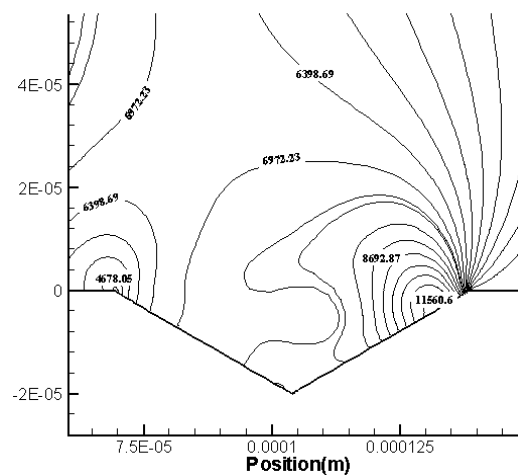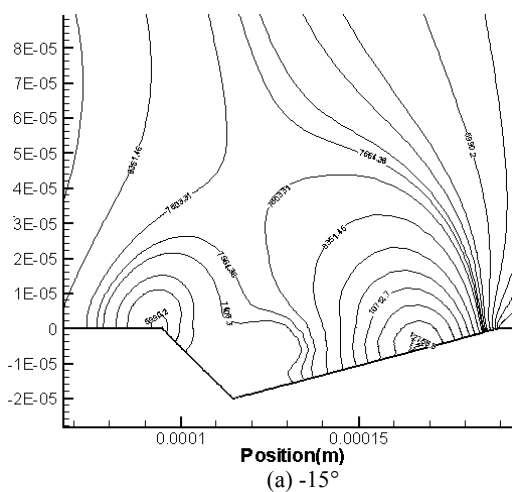

(a) -15°

(b) 0°

(c) 15°

Fig.9 Distribution on static pressure on riblet surfaces with different attitude angles while 0.7M.

Distribution of low pressure zone located at front end of riblet is also affected by the attitude angle. We can see from Fig.9 that value of low pressure center with attitude angle -15° is 5887.2Pa; that of 0° is 4678.1Pa while it is 5373.7Pa with attitude angle 15°. In the CFD results there exists a expansion area from high pressure to low pressure which is closely related to the inner area of riblet grooves and could be affected by the riblet attitude angle. In general, static pressure at wall-near area will change in a specific law along with riblet attitude angle.

Pressure drag resulting from deviation of static pressure on riblet surface will also be affected by riblet attitude angles due to its impact on the distribution of static pressure in turbulent boundary layer. This implies that we could achieve pressure drag reduction through optimization of riblet geometry. So, viscous drag reduction due to the microvortex induced in riblet grooves and the weakened shearing , and the additional force caused by static pressure on riblet surfaces which could be reduce by the optimization of riblet geometry will result in the skin friction reduction on riblet surface, which implies that we could achieve obvious drag reduction in high-speed air flow through riblet surfaces.

Force analysis on riblet surfaces with different attitude angles illustrated in Fig.9 is shown in Tab.2. Microvortex induced in

riblet grooves weakened the wall shearing, correspondingly viscous force would degraded. From Tab.2, we could find riblet attitude angle affected the flow characteristics of microvortex, so viscous force will have fluctuation along with the angle. While 0°, value of viscous force is about0.2N. But it will significantly increase when the angle turns to -15° and 15° with the drag increasing rate 17%-20%. Minimum pressure drag at attitude angle 0° is much smaller that of attitude angles -15° and 15° which pressure drag reduction is about 18.7%-20.8%. Above all, we can find the wall shearing and deviation of static pressure is best appropriate for opitimization of riblet geometry to get maximum drag reduction while 0.7M.

Tab.2 Force analysis on riblet surfaces
with different attitude angles

Riblet Attitude Angle	-15°	0°	15°
Viscous Force(N)	0.24039244	0.19903288	0.2343359
Pressure Force(N)	0.049837634	0.042927042	0.052207634
Total Force(N)	0.29023007	0.24195992	0.28654354

E. Velocity Field

Consider now the viscous sublayer. As known, the transverse velocity profile is linear in this regime. Flow structure alteration of turbulence boundary layer on riblet surface is studied by many labs and researchers. It is widely accepted that the impact of velocity field on riblet surface is the domain factor resulting in microvortex and drag reduction. The velocity takes different form in different part of the riblet surface. Vortical flow in riblet grooves greatly degraded the wall shearing force and viscous force on the riblet area of surface. Also, velocity field in turbulence boundary layer significantly changed on riblet surfaces. At high-speed air flow, the thickness of viscous sublayer is about 10μm regardless of on riblet surface and smooth surface, and becomes a little thinner with the growth of flow rate. Riblets aligned on the surface would not affect the thickness of viscous sublayer. From Fig.10, we can see the thickness of boundary layer on riblet surface and smooth surface which demonstrats the property of linear growth of velocity magnitude along with the increase of the boundary layer thickness is almost the same, about 10μm both. It is considered that flow alteration of turbulence boundary layer on riblet surface will not affect the thickness of boundary layer. Distribution of cross section velocity at 0.4Ma is plotted in Fig.10.
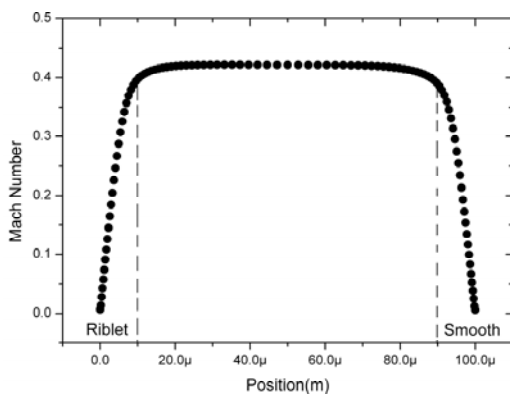

Fig.10 Distribution of cross-section velocity at flow rate 0.4Ma.

Impact of mach number on distribution of cross section velocity field is illustrated in Fig.11.The thickness of turbulent boundary layer will go smaller with the increasing of mach number. The cross-section velocity distribution is all linear regardless of mach number in boundary layer.
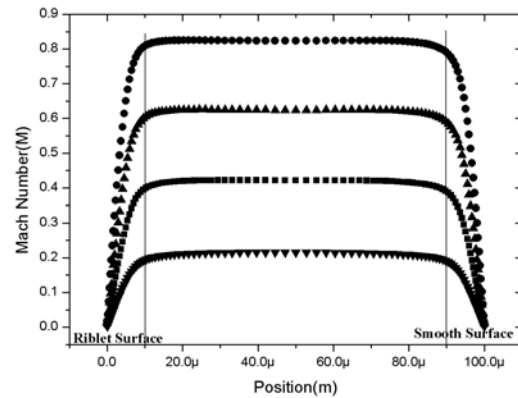

Fig.11 Distribution of cross-section velocity with mach number ranging from 0.2M to 0.8M

The most notable feature on riblet surfaces is the velocity field which has greatly redistributed due to the induced micro −vortex. A number of previous studies have shown that velocity field on riblet surface is closely related to the drag reduction mechanism. Choi et al. (1993) used direct numerical simulation (DNS) to simulate the velocity field over riblets in order to investigate characteristics of flow and its drag reduction mechanism. They found that the drag is reduced due to the relatively small area affected by the down-wash motion of the streamwise vortices and the change of velocity field [19]. Goldstein et al. (1995) attributed the velocity field change to the damping of cross-flow velocity fluctuations. Riblets spaced closely do not allow large streamwise vortices to settle inside the riblet valleys, whereas such vortices can reside in the valleys between widely spaced riblets [22]. With the development of Particle Image Velocimetry Technology, the instantaneous velocity distribution without any contacts to flow could be achieved [23].

We analyzed the influence of riblet surface on the distribution of flow velocity inside the grooves. Fig.12 is presented to illustrate the contours of velocity and along with the locations of the riblets. An obvious vortex generated from the turbulent shear force at the adjacent area of flow inside the grooves and the outer flow, where the value of velocity decreased significantly from 139(m/s) to 16(m/s). Momentum transfer into the vortices on riblet surface is considered happened on this area. It should be noted that the shear action at the groove walls is greatly degraded which is the dominant factor for the drag reduction due to the decreasing linear velocity of the vortex at near wall area. The gradually variational value of velocity is shown in Fig.12.
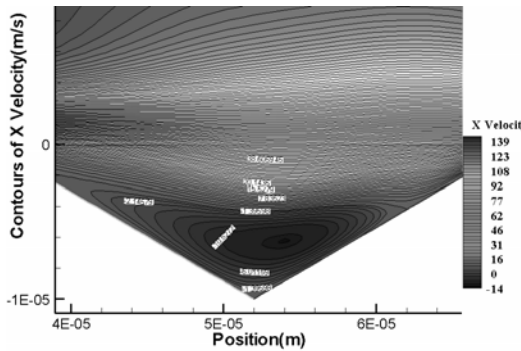
Fig.12 Contours of X_Velocity inside riblet groove at flow rate 0.4Ma.

Riblet attitude angle will also significantly affect the velocity field inside the riblet grooves due to microstructure, which cause alteration of flow structure on riblet surfaces. Impact of three different riblet attitude angles on velocity field has been shown in Fig.13. We can find out microvortex could be induced inside riblet grooves regardless of attitude angle. But the flow characteristics is related to the angles. Especially the distribution of vortex line speed is renewed. In Fig.13, vortical maximum swing speed would gradually degrade along with the angle ranging from -15° to 15°.The value of the speed is about 34m/s while -15° and that is 29m/s while 29m/s. Minimum speed is achieved while the attitude angle is 15°, and the value is 22m/s. Riblet attitude angles has significantly affect the swing speed of microvortex. That is because impinging jet gets much stronger due to the steeper windward side of riblet while -15° which will result in bigger force to form the microvortex in riblet grooves. Further, riblet attitude angles would affect the vortical characteristics of microvortex.

Strong collision when the high-speed air flow impacts the riblet wall will result in higher velocity gradient at front end of riblets than the rear end of riblets, correspondingly stronger shearing force will cause bigger wall friction force at this area. Impact of riblet attitude angles on vortical characteristics and turbulence boundary layer is studied in this paper. Compared with the Fig.13(a),(b),(c), we will find out velocity contour appears obvious sinking at the windward area of riblet while the attitude angle 15°. And, this is considered the reason for the higher pressure distribution at this area with riblet attitude angle15°.
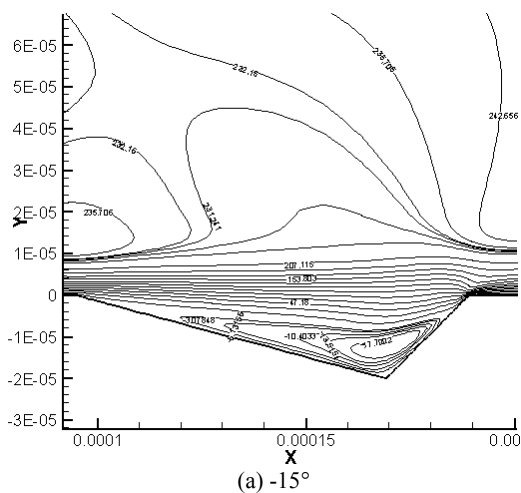
(a) -15°
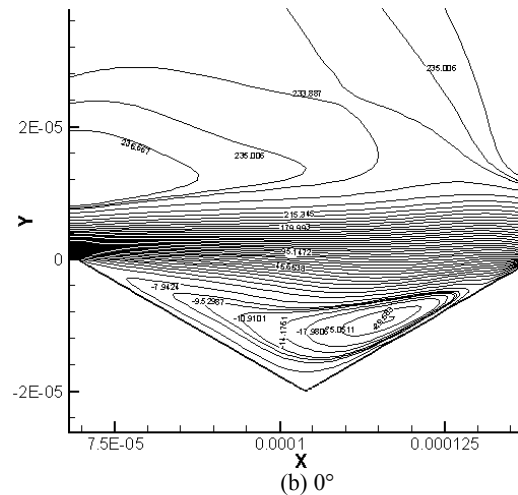
(b) 0°
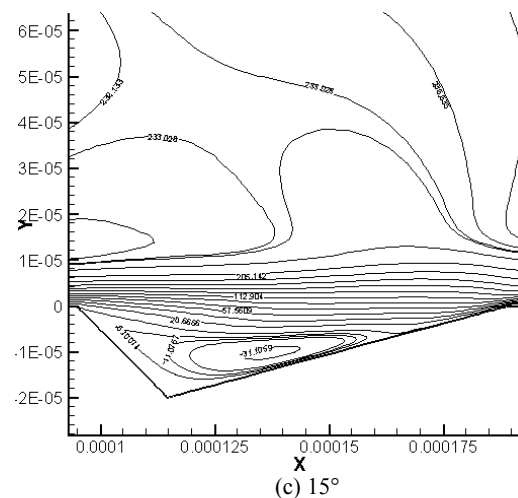
(c) 15°

Fig.13 Velocity field with three different riblet attitude angles on riblet surfaces.

VI. CONCLUSIONs

Research on viscous drag reduction has become vital nowadays due to the shortage of fossil fuel and its high prices. Riblet as one of the successful and reliable passive techniques has been investigated numerically using DNS. The accurate numerical treatment based on k-ε turbulence model for thin triangular riblet surfaces with different riblet attitude angles at high-speed air flow was an efficient method to study the characteristics of flow and drag reduction and increase mechanisms. Several simulation cases have been studied to explore the mechanisms and flow alteration. Microtex induced in riblet grooves will greatly reduce the viscous force and correspondingly pressure force resulting from the deviation of static pressure will be caused . Force analysis on riblet surface was carried on in this paper.With the triangular riblet aligned on the surface, the shear stress is significantly decreased exhibiting an obvious valley on the curve in Fig.5(a) and Fig.6(a), which is considered the dominant factor resulting in drag reduction.The additional force generating from the deviation of static pressure on the front and rear end of the riblet groove caused pressure drag increasing with the flow rate. Also, static pressure and velocity field on riblet surface with

different riblet attitude angles are studied. The results shows riblet attitude angle will significantly affect the flow characteristics. The proposed numerical treatment is a useful and efficient technique for triangular riblet surfaces on drag reduction mechanisms and flow structure analysis.

REFERENCES

[1] Suzuki, Yuji, and Kasagi,"Turbulent drag reduction mechanism above a riblet surface, " *AIAA Journal*, vol.32, no.9, pp. 1781-1790,1994.

[2] García-Mayoral, Ricardo , and Jiménez, Javier, "Drag reduction by riblets," *Philosophical Transactions of the Royal Society A: Mathematical, Physical and Engineering Sciences*, vol.369, no.1940, pp. 1412-1427,2011.

[3] Vukoslavcevic, J.M. Wallace, and J.L. Balint, "Viscous drag reduction using streamwise- aligned riblets, "*AIAA Journal*, vol.350, no.30, pp. 1119-1122,1992.

[4] S.-R. Park, and J.M. Wallace, "Flow alteration and drag reduction by riblets in a turbulent boundary layer," *AIAA Journal*, vol.352, no.32, pp. 31-38, 1994.

[5] Okamoto Shiki,Yoshisaki Takashi,and Kobayashi Masato, "Drag reduction in pipe flow with riblet, "*Nippon Kikai Gakkai Ronbunshu, B Hen/Transactions of the Japan Society of Mechanical Engi*neers, *Part B*, vol.68, no.668, pp. 1058-1064,2002.

[6] Zhang H.Y.,Yang H.X.,and Li G., "Numerical study of turbulent drag reduction over riblet surface, " *Proceedings of the International Offshore and Polar Engineering Conference*, pp. 441-445,2008.

[7] O.A. El-Samna, H.H. Chun, and H.S. Yoon, "Drag reduction of turbulent flow over thin rectangular riblets, " *International Journal of Engineering Science*, no.45, pp. 436-454,2007.

[8] Jiménez, and Javier, "Turbulent flows over rough walls," *Annual Review of Fluid Mechanics*, vol.36, pp. 173-196, 2004.

[9] Peet Yulia, and Sagaut Pierre, "Theoretical prediction of turbulent skin friction on geometrically complex surfaces," *Physics of Fluids*, vol.21, no.10, Article number: 105105, 2009.

[10] Bechert D.W.,Bruse M., Hage W.,and Van der Hoeven J.G.T., "Experiments on drag-reducing surfaces and their optimization with an adjustable geometry, " *Journal of Fluid Mechanics*, vol.338, pp. 59-87,1997.

[11] Grüneberger René, and Hage Wolfram, "Drag characteristics of longitudinal and transverse riblets at low dimensionless spacings," *Experiments in Fluids*, vol.50, no.2, pp. 363-373,2011.

[12] Fang Yihong,Liu Yifang,Ye Xingfu, "Existence of shocklets in supersonic boundary layer and its relation with 3-D disturbance, " *2nd WSEAS International Conference on Fluid Mechanics and Heat and Mass Transfer,*pp. 152-157,2011

[13] Joseph, D. D. and Y. Renardy, "Fundamentals of Two-Fluid Dynamics. Part 1: Mathematical Theory and Applications, " New York: Springer -Verlag, 1993.

[14] Sheikhy Nasrin,Bahrami Milad,Rahimi Asghar B., "Analyzing the cross section effect of hypersonic flow past a conical body via perturbation method", *Proc. IASME / WSEAS Int. Conf. Fluid Mech. Aerodyn.,*pp. 182-187.2009.

[15] Beghidja, A., Gouidmi, H., Benderradji, R., "Study of the interaction shock wave boundary layer with the K-ω turbulence model, " *WSEAS Trans. Inf. Sci. Appl,*vol.3,no.5,pp. 921-926,2006.

[16] D.D. Joseph, and C. Christodoulou, "Independent confirmation that delayed die swell is a hyperbolic transition," *J. Non-Newtonian Fluid Mech.*, vol.48, no.3, pp. 225-235, 1995.

[17] KE Feng, LIU Ying-zheng, JIN Chun-yu, and WANG Wei-zhe, "Experimental measurements of turbulent boundary layer flow over a square-edged rib," *Conference of Global Chinese Scholars on Hydrodynamics,* pp.461-464, 2006.

[18] Luchini P, Manzo F, and Pozzi A. " Resistance of a grooved surface to parallel flow and cross flow, " *J Fluid Mech*, pp. 87–109,1981.

[19] Choi, H.C., Moin, P., and Kim, J. "Direct Numerical Simulation of turbulent flow over riblets," *Journal of Fluid Mechanics,* pp.503－539,1993.

[20] McLean JD, George-Falvy DN, and Sullivan PP. "Flight-tes t of turbulent skin friction reduction by riblets," *Proceedings of International Conference on Turbulent Drag Reduction by Passive Means*, London: Royal Aeronautical Society, pp.1-17,1987.

[21] Walsh MJ, and Sellers WL. "Riblet drag reduction at flight conditions. "*AIAA Paper* ,No:88-2554, 1988.

[22] Goldstein, D., Handler, R., and Sirovich, L., "Direct Numerical Simulation of turbulent flow over a modeled riblet covered surface," *Journal of Fluid Mechanics*, pp.333－376,1995.

[23] Kawasue Kikuhito,Aramaki Satoshi1, and Ohya, Yuichiro, "Calibration -free PIV system using magnetic sensors," *WSEAS Trans. Syst*, pp.2737 -2743,2006.